Cancer Cell
Article

Hepatic Stem-like Phenotype and Interplay of Wnt/β-Catenin and Myc Signaling in Aggressive Childhood Liver Cancer

Stefano Cairo,[1,2,30] Carolina Armengol,[1,2,30] Aurélien De Reyniès,[3] Yu Wei,[1,2] Emilie Thomas,[3] Claire-Angélique Renard,[1,2] Andrei Goga,[4] Asha Balakrishnan,[4] Michaela Semeraro,[5] Lionel Gresh,[6] Marco Pontoglio,[6] Hélène Strick-Marchand,[7] Florence Levillayer,[1,2] Yann Nouet,[1,2] David Rickman,[3] Frédéric Gauthier,[8] Sophie Branchereau,[8] Laurence Brugières,[9] Véronique Laithier,[10] Raymonde Bouvier,[11] Françoise Boman,[12] Giuseppe Basso,[13] Jean-François Michiels,[14] Paul Hofman,[15] Francine Arbez-Gindre,[16] Hélène Jouan,[17] Marie-Christine Rousselet-Chapeau,[18] Dominique Berrebi,[19] Luc Marcellin,[20] François Plenat,[21] Dominique Zachar,[22] Madeleine Joubert,[23] Janick Selves,[24] Dominique Pasquier,[25] Paulette Bioulac-Sage,[26] Michael Grotzer,[27] Margaret Childs,[28] Monique Fabre,[29] and Marie-Annick Buendia[1,2,*]

[1]Oncogenesis and Molecular Virology Unit, Institut Pasteur, 28 rue du Docteur Roux, 75724 Paris Cedex 15, France
[2]INSERM U579, 28 rue du Docteur Roux, 75724 Paris Cedex 15, France
[3]Programme Cartes d'Identité des Tumeurs, Ligue Nationale Contre le Cancer, 75013 Paris, France
[4]Division of Hematology/Oncology, University of California, San Francisco, San Francisco, CA 94143-1270, USA
[5]Histotechnology and Pathology Unit, Institut Pasteur, 75724 Paris Cedex 15, France
[6]Gene Expression Development and Disease Unit, Centre National de la Recherche Scientifique URA 2578, Institut Pasteur, 75724 Paris Cedex 15, France
[7]Cytokine and Lymphoid Development Unit, Immunology Department, Institut Pasteur, 75724 Paris Cedex 15, France
[8]Service de Chirurgie Pédiatrique, Centre Hospitalo-Universitaire de Bicêtre APHP, 94275 Le Kremlin-Bicêtre, France
[9]Department of Pediatric Oncology, Institut Gustave Roussy, 94800 Villejuif, France
[10]Pediatric Hematology Oncology Service, Centre Hospitalier Universitaire Saint Jacques, 25030 Besançon, France
[11]Service d'Anatomie et Cytologie Pathologiques, Centre Hospitalier Universitaire, Hôpital Edouard Herriot, 69003 Lyon, France
[12]Pôle de Pathologie, Centre Biologie-Pathologie, CHRU de Lille, 59000 Lille, France
[13]Department of Pediatrics, University of Padova, 35128 Padova, Italy
[14]Laboratoire Central d'Anatomie Pathologique, Hôpital Pasteur, Centre Hospitalier Universitaire de Nice, 06000 Nice, France
[15]INSERM ERI-21, Faculty of Medicine and Laboratory of Clinical and Experimental Pathology, Pasteur Hospital, 06000 Nice, France
[16]Service d'Anatomie et de Cytologie Pathologiques, Centre Hospitalier Universitaire Jean Minjoz, 25030 Besançon, France
[17]Département d'Anatomopathologie, Centre Hospitalier de Pontchaillou, 35000 Rennes, France
[18]Laboratoire d'Anatomie Pathologique, Centre Hospitalier Universitaire, et Laboratoire HIFIH, UPRES 859, IFR 132, Université d'Angers, 49100 Angers, France
[19]Anatomie et Cytologie Pathologiques, Hôpital Robert Debré, 75019 Paris, France
[20]Service d'Anatomie Pathologique Générale, Hôpital de Hautepierre, 67098 Strasbourg, France
[21]Department of Pathology, CHU Nancy-Brabois, 54511Vandoeuvre, France
[22]Laboratoire Pol Bouin, Hôpital Maison Blanche, 51100 Reims, France
[23]Anatomie et Cytologie Pathologiques, Centre Hospitalier Universitaire de Nantes, 44093 Nantes, France
[24]Laboratoire d'Anatomie et Cytologie Pathologiques, Hôpital Purpan, 31059 Toulouse, France
[25]Service d'Anatomie Pathologique, Centre Hospitalier Universitaire A. Michallon, 38043 Grenoble, France
[26]Department of Pathology, CHU Bordeaux, INSERM U889, Université Victor Segalen Bordeaux 2, 33076 Bordeaux, France
[27]SIOPEL Tumor Banking Program, University Children's Hospital, 8032 Zurich, Switzerland
[28]Children's Cancer and Leukaemia Group Data Centre, University of Leicester, LE1 7RH Leicester, UK
[29]Service d'Anatomie et de Cytologie Pathologiques, Université Paris-Sud 11, APHP Hôpital de Bicêtre, 94275 Le Kremlin-Bicêtre, France
[30]These authors contributed equally to this work
*Correspondence: mbuendia@pasteur.fr
DOI 10.1016/j.ccr.2008.11.002

SIGNIFICANCE

The role of Wnt signaling in liver development and tumorigenesis remains elusive. Here we investigated the pathogenesis of hepatoblastoma, a pediatric tumor strongly associated with mutational activation of β-catenin. By integrating expression and genetic profiles of clinically annotated tumors, we provide a molecular overview of a previously unrecognized prognostic subtype that evokes cancer stem/progenitor cells. Activation of Myc might play a predominant role in the pathogenesis of this tumor subtype. We demonstrate that hepatic differentiation stage and clinical behavior of hepatoblastoma are intimately linked, and we identify an expression signature with dual capacities in recognizing liver developmental stage and predicting disease outcome. These data can be applied to improve clinical management of pediatric liver cancer and develop therapeutic strategies.

SUMMARY

Hepatoblastoma, the most common pediatric liver cancer, is tightly linked to excessive Wnt/β-catenin signaling. Here, we used microarray analysis to identify two tumor subclasses resembling distinct phases of liver development and a discriminating 16-gene signature. β-catenin activated different transcriptional programs in the two tumor types, with distinctive expression of hepatic stem/progenitor markers in immature tumors. This highly proliferating subclass was typified by gains of chromosomes 8q and 2p and upregulated Myc signaling. Myc-induced hepatoblastoma-like tumors in mice strikingly resembled the human immature subtype, and Myc downregulation in hepatoblastoma cells impaired tumorigenesis in vivo. Remarkably, the 16-gene signature discriminated invasive and metastatic hepatoblastomas and predicted prognosis with high accuracy.

INTRODUCTION

Fine-tuned control of Wnt/β-catenin signaling is essential for cellular proliferation and proper differentiation during development and tissue homeostasis, and its forced deregulation leads to malignant transformation of various cell types. Recently, a major role has been assigned to the Wnt/β-catenin pathway in maintenance of tissue-specific stem cells and proliferation of epithelial progenitor cells (Korinek et al., 1998; Lowry et al., 2005). While the role of Wnt signaling at initial steps of liver organogenesis remains elusive (McLin et al., 2007; Ober et al., 2006), this pathway stimulates proliferation of the developing liver and governs metabolic zonation and essential hepatic functions (Benhamouche et al., 2006; Micsenyi et al., 2004). Furthermore, aberrant deregulation of Wnt signaling has been implicated as a major mechanism of liver tumorigenesis (de La Coste et al., 1998).

The cancer stem cell hypothesis surmises that most tumor cell populations are derived from rare undifferentiated cells with stem-like capabilities of self-renewal and differentiation (Reya et al., 2001). Liver cancer stem/progenitor cells have been isolated from human hepatoma cell lines and primary hepatocellular carcinomas (HCCs) (Ma et al., 2007; Yang et al., 2008), and convincing support has been provided for the notion that some HCC subtypes are derived from hepatic progenitors (Lee et al., 2006; Yamashita et al., 2008; Zender et al., 2005). The mechanisms leading to malignant transformation of stem/progenitor cells can be effectively addressed in pediatric tumors. Hepatoblastoma (HB) is a malignant embryonal tumor of the liver usually diagnosed in children younger than 3 years of age (Schnater et al., 2003; Weinberg and Finegold, 1983). In the absence of underlying liver disease or viral infection, evidence for genetic/epigenetic origin of this tumor is provided by increased risk associated with congenital anomalies, Beckwith-Wiedemann syndrome, and familial adenomatous polyposis (FAP), a disorder caused by germline mutations of the *APC* gene involved in β-catenin degradation. A further link between HB genetics and the Wnt/β-catenin pathway is provided by the high rate (50%–90%) of mutations found in *CTNNB1*, which encodes β-catenin, placing HB among the most common human tumors endowed with constitutive activation of β-catenin/Tcf signaling (Koch et al., 1999; Taniguchi et al., 2002; Wei et al., 2000). HB differs from HCC by distinctive morphological patterns reminiscent of hepatoblasts, the bipotent precursors of hepatocytes and cholangiocytes, and of their arrangement in the developing liver (Ishak and Glunz, 1967). Histologically, HB is classified into different patterns, including the frequent fetal pattern that evokes the prenatal fetal liver with sheets of uniform, cuboidal cells showing low mitotic activity; the more immature embryonal type characterized by higher cell density, enlarged nuclei, and frequent mitosis; macrotrabecular patterns evoking HCC; and small cell undifferentiated (SCUD) pattern, suggesting that HB may arise from a primitive, uncommitted progenitor (Zimmermann, 2005). Additionally, admixed neoplastic mesenchymal derivatives and occasional teratoid features in mixed-type HBs (20%–40% of cases) suggest multidirectional differentiation abilities of tumor cells.

Although HB is the predominant type of liver cancer in young children, this tumor is rare, comprising 1% of total pediatric malignancies. During the last decades, large international clinical trials have improved the prognosis of HB patients, resulting currently in 5-year survival rates averaging 75% (Ortega et al., 2000; Perilongo et al., 2000; Schnater et al., 2003). Complete surgical resection or liver transplantation and mainstream treatment with cytotoxic drugs are essential for achieving favorable long-term outcome. Despite diverse staging systems worldwide, common prognostic factors rely on intrahepatic tumor extension, multifocality, invasion of liver vessels, and distant metastases (Perilongo et al., 2000), whereas prognostic significance of histopathologic criteria remains debated. At present, few studies have addressed whether intrinsic biological differences between tumors impact HB prognosis. Moreover, new treatments are urgently needed for advanced-stage tumors, and better understanding of HB pathobiology is a prerequisite for developing targeted therapies.

To gain a comprehensive view of HB pathogenesis, the current study combined gene expression and array-based comparative genomic hybridization (aCGH) analysis of clinically annotated tumors with functional studies in cell lines and murine liver tumors.

RESULTS

Evidence of Wnt/β-Catenin Activation by Genetic and Transcriptional Profiling

Gene expression and genetic changes were analyzed in 102 clinically annotated tumor samples from 85 patients (see Tables S1 and S2 available online). We started with a genetic screen of *CTNNB1*, *AXIN1*, and *AXIN2*, genes that are frequently mutated in liver cancer. *CTNNB1* mutations were detected in 65 cases (76%). Four cases were from FAP kindreds, indicating germline mutation of the *APC* gene; *AXIN1* was mutated in 1 of 61 cases analyzed; and *AXIN2* was wild-type. In total, 82% of tumors harbored genetic mutations related to the Wnt pathway (Table S1).

Twenty-five representative HB samples from 24 patients and 4 nontumor liver samples were profiled via Affymetrix HG-U133A microarrays. Analysis of differentially expressed genes between tumor and nontumor samples confirmed involvement of Wnt signaling as reported in previous studies (Koch et al., 1999, 2005; Wei et al., 2000) (Table S3). More specifically, we found upregulation of Wnt signaling components implicated in feedback regulations like *AXIN2*, the positive effectors *LEF1*, *DVL2*, and *DVL3*, and the Wnt antagonists *DKK1* and *DKK4*. Moreover, a significant number of genes upregulated in HB such as *GLUL* (encoding glutamine synthetase) and *TBX3* are selectively overexpressed in human and murine HCCs carrying mutant β-catenin (Boyault et al., 2007; Stahl et al., 2005) (Table 1). We used gene lists from these two previous studies to perform gene set enrichment analysis (GSEA), a computational method for assessing enrichment of a predefined gene list in one class as compared with another (Subramanian et al., 2005). This analysis revealed that β-catenin-related genes in HCC were significant enriched in HB versus normal liver (Figure S1; Table S4). Pathway and Gene Ontology (GO) analysis confirmed deregulation of Wnt signaling and indicated downregulation of genes involved in liver functions such as metabolism of amino acids, steroids, fatty acids, glucose, xenobiotics, and alcohol and the complement and coagulation cascade (Tables S5 and S6). Another clear observation was the strong upregulation of several imprinted genes such as *IGF2*, *DLK1*, *PEG3*, *PEG10*, *BEX1*, *MEG3*, and *NDN*, which are abundantly expressed in fetal liver (Figure S2).

Identification of Two HB Subclasses by Gene Expression Profiling

For robust unsupervised classification, we generated and screened a series of 24 dendrograms to identify samples that coclustered irrespective of the method and the gene list used (see Supplemental Experimental Procedures). We obtained two robust subgroups of tumors, named robust Cluster 1 (rC1, n = 8) and robust Cluster 2 (rC2, n = 5) (Figure 1A). Comparison of rC1 and rC2 expression profiles identified 824 genes ($p < 0.001$, false discovery rate [FDR] = 0.02) (Table S7). Pathway and GO analysis pinpointed enrichment in rC2 tumors of cell-cycle-related genes, particularly spindle checkpoint genes such as *DLG7*, *CDC2*, *BUB1*, and *AURKB* (Tables S8 and S9), which are also activated in human embryonic stem cells and in aggressive tumors (Assou et al., 2007). Evidence that rC2 tumors were faster proliferating than rC1 tumors was confirmed by Ki-67 immunostaining (see Figure 2A).

To classify the remaining tumors, we built a sample classifier based on the expression of 16 of the most differentially expressed genes between rC1 and rC2 at $p < 10^{-7}$ and the 13 robust cluster samples to train the classifier (Figure 1A; Table S10). Most of these genes showed drastic variations in expression level during liver development, such as *AFP* and the proliferation markers *BUB1* and *DLG7*. When the signature was employed to classify the remaining tumors into C1 (rC1-related) and C2 (rC2-related) subclasses, the same classification was obtained using microarray or quantitative PCR (qPCR) (Figure 1B; Table S11). Because most patients (19 of 24) received preoperative chemotherapy, we verified that sample distribution was independent of previous treatment. Principal component analysis (PCA) clearly showed that chemotherapy-treated and untreated samples were evenly distributed (Figure S3). Both groups exhibited similar, high rates of β-catenin mutations, and most tumors showed cytoplasmic and nuclear staining of the protein. However, β-catenin localization was predominantly membranous and cytoplasmic in C1 tumors, whereas it showed frequent loss of membrane anchoring and intense nuclear accumulation in C2 tumors (Figure 1B). We observed differential expression of a number of Wnt members and targets between subclasses. C2 tumors showed increased expression of *MYCN*, *BIRC5* (encoding survivin), *NPM1*, *HDAC2*, and stem cell-related genes such as *TACSTD1* (encoding Ep-CAM), *GJA1*, and the polycomb gene *SUZ12* (Table 1). Conversely, C1 showed overexpression of genes related to the liver perivenous area, such as *GLUL*, *RHBG*, and two members of the cytochrome p450 family, *CYP2E1* and *CYP1A1* (Benhamouche et al., 2006; Braeuning et al., 2006) (Table 1; Figure 1C). GSEA further indicated that the rC1 subclass was enriched in genes assigned to the hepatic perivenous program (Table S12). Thus, Wnt/β-catenin signaling appears to activate different transcriptional programs in HB subtypes.

HB Subclasses Evoke Distinct Phases of Liver Development

Next, we sought to determine whether HB subclasses were associated with specific histological phenotypes. Mixed epithelial-mesenchymal tumors in 20% of cases were not significantly associated with C1 and C2 subclasses. By contrast, a tight association was found with the main epithelial component, which defines the epithelial cell type occupying more than 50% of tumor cross-sectional areas. C1 tumors displayed a predominantly fetal phenotype, including four "pure fetal" cases, whereas C2 tumors showed a more immature pattern, with prevailing embryonal or crowded fetal histotypes associated with high proliferation ($p < 0.0001$) (Figure 2A). Accordingly, mature hepatocyte markers were markedly downregulated in C2 compared to C1 tumors (Figure 2B; Table S7), and strong overexpression of the hepatic progenitor markers *AFP*, *KRT19*, and *TACSTD1* was found in C2 HBs (Figures 2A and 2B).

To better define the relationships between HB subclasses and phases of hepatic differentiation, we first generated a liver development-related gene signature using available mouse liver data sets (Otu et al., 2007) (Table S13). When applied to HB samples, this signature was able to distinguish by hierarchical clustering two HB groups closely matching the C1/C2 classification (Figure S4). Next, we integrated HB gene expression data with the orthologous genes expressed in mouse livers at embryonic days 11.5–18.5 (E11.5–E18.5) and at 8 days after birth. In unsupervised clustering, most C2 tumors coclustered with mouse livers at early stages of embryonic development (E11.5 and E12.5), whereas C1 tumors gathered with mouse livers at late fetal and postnatal stages (Figure 2C), supporting the notion that HB subtypes mimic different points of the hepatic differentiation program.

Gains on Chromosomes 8 and 2 Are Associated with the C2 Subclass

To explore whether genetic abnormalities might be implicated in the pathogenesis of the HB subclasses, 24 of the 25 tumors examined by expression profiling were analyzed by aCGH. Recurrent chromosomal aberrations consisted of gains on chromosomes 1q (71%), 2q (54%), 6p (25%), 8q (25%), and 20 (21%)

Table 1. β-Catenin Target Genes Significantly Deregulated in HB

Probe Set	Gene Symbol	Gene Name	Fold Change HB/NL	Fold Change rC1/rC2	Reference
Ubiquitous Targets					
–	*AXIN2*	axin 2 (conductin, axil)	up[a]	NS	–
204602_at	*DKK1*	dickkopf homolog 1 (*X. laevis*)	20.2	NS	–
221558_s_at	*LEF1*	lymphoid enhancer-binding factor 1	4.8	1.2	–
203304_at	*BAMBI*	BMP and activin membrane-bound inhibitor homolog (*X. laevis*)	3.0	NS	Sekiya et al. (2004)
211518_s_at	*BMP4*	bone morphogenetic protein 4	3.0	2.2	–
209589_s_at	*EPHB2*	EPH receptor B2	2.0	1.2	–
221923_s_at 200063_s_at	*NPM1*	nucleophosmin (nucleolar phosphoprotein B23, numatrin)	1.8	0.5	–
202095_s_at	*BIRC5*	baculoviral IAP repeat-containing 5 (survivin)	NS	0.2	–
Stem Cell-Related Targets					
201839_s_at	*TACSTD1*	tumor-associated calcium signal transducer 1	9.7	0.2	Yamashita et al. (2007)
213880_at 210393_at	*LGR5*	leucine-rich repeat-containing G protein-coupled receptor 5	8.5	NS	–
201667_at	*GJA1*	gap junction protein, alpha 1, 43kDa (connexin 43)	3.8	NS	–
219682_s_at	*TBX3*	T-box 3 (ulnar mammary syndrome)	3.5	NS	Renard et al. (2007)
212287_at 213971_s_at	*SUZ12*	suppressor of zeste 12 homolog (*Drosophila*)	1.7	0.7	Kirmizis et al. (2003)
202936_s_at 218310_at	*SOX9*	SRY (sex determining region Y)-box 9 (campomelic dysplasia, autosomal sex-reversal)	NS	0.3	–
Hepatic Targets					
205815_at	*REG3A*	regenerating islet-derived 3 alpha (pancreatitis-associated protein)	15.9	8.6	Cavard et al. (2006)
200648_s_at 217202_s_at 215001_s_at	*GLUL*	glutamate-ammonia ligase (glutamine synthetase)	4.7	3.4	Cadoret et al. (2002)
202479_s_at 202478_at	*TRIB2*	tribbles homolog 2 (*Drosophila*)	4.6	NS	Boyault et al. (2007)
218704_at	*RNF43*	ring finger protein 43	3.8	NS	Boyault et al. (2007)
220510_at	*RHBG*	rhesus blood group, B glycoprotein	3.0	NS	Boyault et al. (2007)
201833_at	*HDAC2*	histone deacetylase 2	2.0	0.5	Benhamouche et al. (2006)
205244_s_at 205243_at	*SLC13A3*	solute carrier family 13 (sodium-dependent dicarboxylate transporter), member 3	1.8	NS	Boyault et al. (2007)
204310_s_at	*NPR2*	natriuretic peptide receptor B/guanylate cyclase B	1.8	NS	Boyault et al. (2007)
205749_at	*CYP1A1*	cytochrome P450, family 1, subfamily A, polypeptide 1	0.3	3.1	Braeuning et al. (2006)
1431_at 209975_at 209976_s_at	*CYP2E1*	cytochrome P450, family 2, subfamily E, polypeptide 1	NS	4.5	Braeuning et al. (2006)
208389_s_at	*SLC1A2*	solute carrier family 1 (glial high-affinity glutamate transporter), member 2	NS	1.7	Stahl et al. (2005)
Wnt Pathway-Related Genes					
209220_at	*GPC3*	glypican 3	19.5	NS	Capurro et al. (2005)
202196_s_at 214247_s_at	*DKK3*	dickkopf homolog 3 (*X. laevis*)	5.4	8.6	Yue et al. (2008)
201908_at	*DVL3*	dishevelled, dsh homolog 3 (*Drosophila*)	1.9	NS	–
57532_at	*DVL2*	dishevelled, dsh homolog 2 (*Drosophila*)	1.7	NS	–

Table 1. *Continued*

Probe Set	Gene Symbol	Gene Name	Fold Change HB/NL	Fold Change rC1/rC2	Reference
202036_s_at	*SFRP1*	secreted frizzled-related protein 1	0.8	NS	–
207468_s_at	*SFRP5*	secreted frizzled-related protein 5	0.7	NS	–
206737_at	*WNT11*	wingless-type MMTV integration site family, member 11	0.7	1.3	–

When genes have more than one probe set, mean expression ratios are shown. $p < 0.05$ was considered significant. NS, no significant change. Unless otherwise specified, references are available at the Wnt Homepage (http://www.stanford.edu/~rnusse/wntwindow.html).
[a] Assessed by qPCR (fold change = 149.1) in the absence of the *AXIN2* probe set on U133A arrays.

and losses on 1p (37%) and 4q (33%). Five tumors, of which four were classified as C1, displayed no large regional change. Interestingly, the frequency of DNA copy gains was elevated by 3-fold in the C2 subclass, with specific involvement of chromosomes 2 and 8 (Figures 3A and 3B). Three regions of chromosome 2 were significantly gained in the C2 subclass, including 2q13-q22, 2q36-37, and the entire 2p arm. In particular, four C2 tumors, but no C1 tumors, gained the 2p arm. The strongest difference was observed for chromosome 8, with gain of the long arm or whole chromosome in 6 of 7 C2 tumors, whereas no 8/8q gain was observed in C1 tumors ($p < 0.00005$).

The impact of genomic differences on gene expression was evaluated by GSEA, which showed significant upregulation of genes localized on chromosomes 2p and 8q in C2 tumors (Figure 3C; Tables S14 and S15). Next, we checked the expression of two Myc-family oncogenes, *MYCN* and *MYC*, which map to chromosomes 2p24.1 and 8q24.21. Using microarray data, we found increased expression of *MYCN* in C2 tumors, while *MYC* expression was upregulated in C2 versus C1 HBs but was not significantly different compared to nontumor livers (Figure 3D). The impact of Myc expression was investigated by GSEA using a list of 88 Myc-upregulated target genes validated by chromatin immunoprecipitation (Zeller et al., 2003). A strong enrichment of Myc target genes was observed in the C2 subclass, with 66% of target genes found to be upregulated (Figure 3E; Table S16). Thus, C2 tumors are characterized by specific chromosomal gains and activation of Myc signaling.

Effects of Aberrant Activation of β-Catenin or Myc on Differentiation and Tumorigenicity of Murine Hepatoblasts In Vitro

To gain more insight into the oncogenic role of β-catenin and Myc-family genes in hepatic progenitor cells, we used murine hepatoblast BMEL cell lines that present features of bipotential

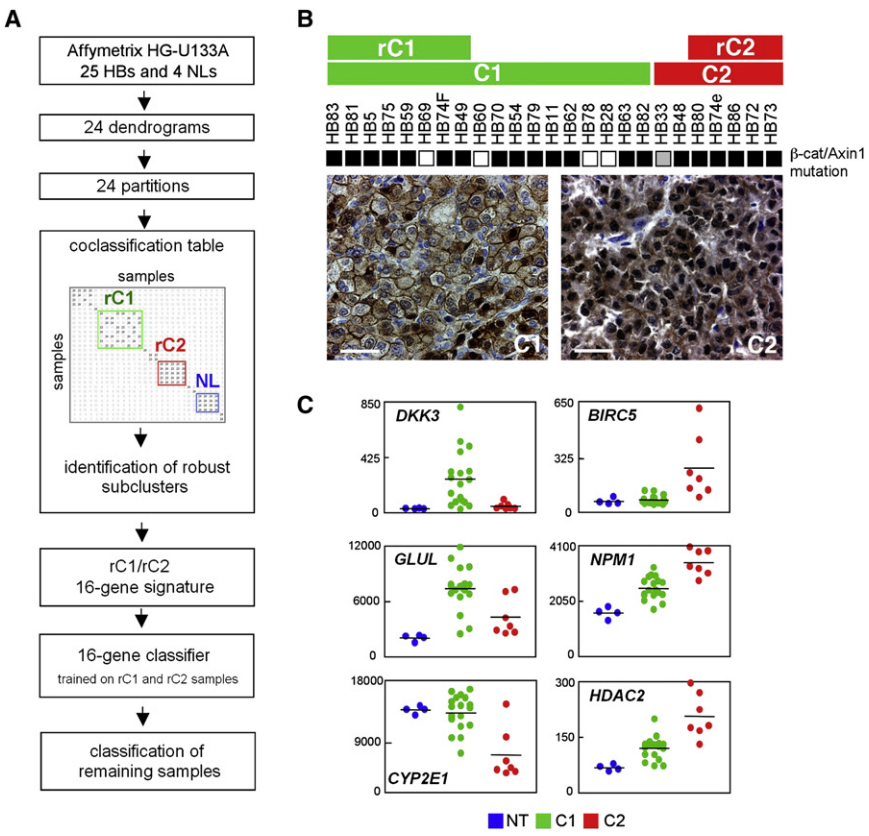

Figure 1. Identification of Two Hepatoblastoma Subclasses by Expression Profiling

(A) Schematic overview of the approach used to identify robust clusters of samples, including two tumor clusters (rC1 and rC2) and one nontumor cluster (NL), and to classify hepatoblastoma (HB) samples using six different algorithms (CCP, LDA, 1NN, 3NN, NC, and SVM) and leave-one-out cross-validation.

(B) Top: molecular classification of 25 HB samples and *CTNNB1* gene status. Black and gray squares indicate mutations of the *CTNNB1* and *AXIN1* genes. Bottom: immunohistochemical analysis of β-catenin for representative C1 and C2 cases. Scale bars = 50 μm.

(C) Expression of representative Wnt-related and β-catenin target genes ($p < 0.005$) in HB subclasses and nontumor livers (NT). Horizontal bars indicate mean values.

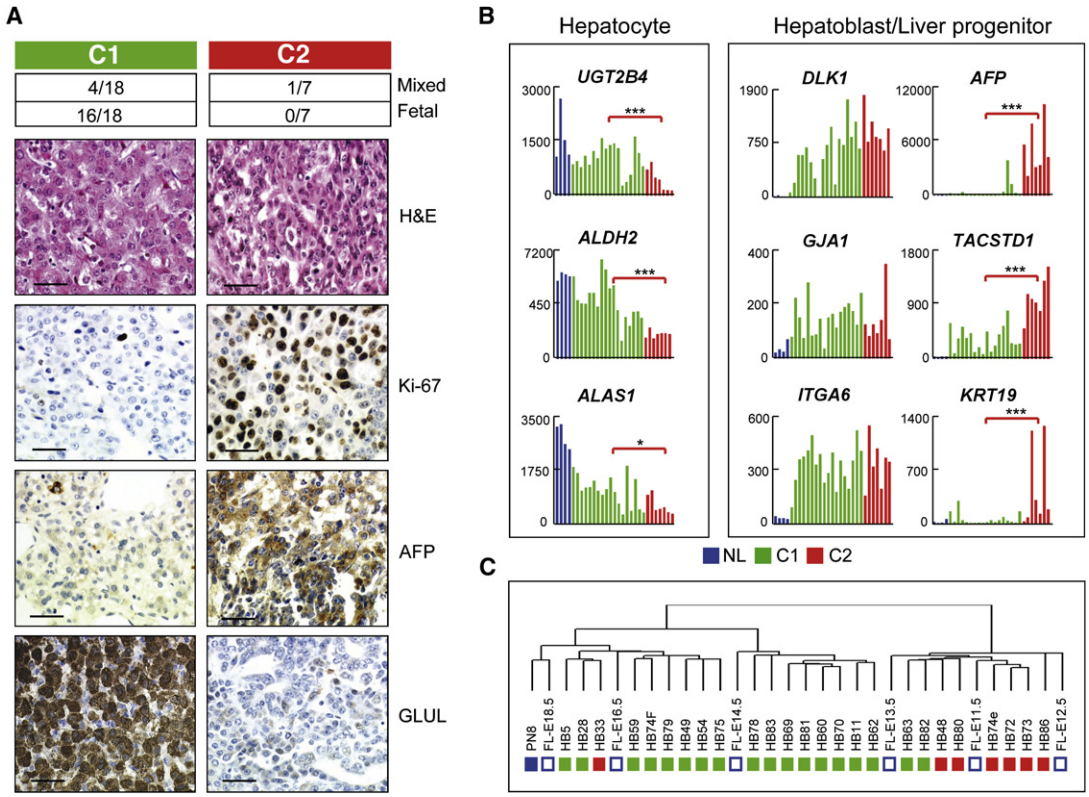

Figure 2. HB Molecular Subclasses Are Related to Liver Development Stages

(A) Distinctive histologic and immunostaining patterns of HB subclasses C1 and C2. From top to bottom: numbers indicate the ratios of mixed epithelial-mesenchymal tumors and tumors with predominantly fetal histotype in C1 and C2 subtypes; hematoxylin and eosin (H&E) and immunostaining of Ki-67, AFP, and GLUL in representative samples. Scale bars = 50 μm.

(B) Expression of selected markers of mature hepatocytes and hepatoblast/liver progenitors in HB subclasses and human nontumor livers (NL). Red brackets indicate statistical comparison of expression levels in C1 and C2 subtypes (*$p < 0.05$, **$p < 0.005$, ***$p < 0.0005$).

(C) Representative unsupervised hierarchical clustering of integrated gene expression profiles from human tumors and mouse livers at different developmental stages. PN8, mouse liver at 8 days after birth; FL, fetal mouse liver (E11.5–E18.5); HB, hepatoblastoma.

embryonic liver stem cells (Strick-Marchand and Weiss, 2002). BMEL-9A1 cell lines stably expressing either active mutant β-catenin or N-myc were generated, and c-Myc was transduced into BMEL lines 9A1 and 14B3 by adenoviral vector (Figure S5A). Analysis of the 16-gene expression profile by qPCR followed by classification using the six algorithms assigned a C1-like expression profile to control BMEL cells (Figure S5B; Table S17). By contrast, marked expression changes leading to classification as C2-type were seen in cells overexpressing β-catenin or Myc genes, with marked downregulation of the hepatocyte markers *Aldh2*, *Apcs*, and *Apoc4* in β-catenin-transduced cells and pronounced upregulation of proliferation-related genes such as *Bub1* and *Dlg7* in Myc-overexpressing cells (Figure 4A).

Functional correlates of these changes were explored by comparing the capacity of these BMEL lines to respond to differentiation and growth signals. BMEL cells can be induced to express markers of normal hepatocyte function when cultured as aggregates (Strick-Marchand and Weiss, 2002). The different stable cell lines were induced to form aggregates by 5-day incubation in nonadherent conditions, and expression of hepatocyte-specific markers was compared between basal cultures and aggregates by qPCR. In control BMEL cells, expression of these genes was strongly activated in aggregates compared with basal conditions, while overexpression of β-catenin or N-myc drastically impaired induction (Figure 4B). We next tested whether overexpression of β-catenin or N-myc might confer anchorage-independent growth properties to these cells. In soft-agar experiments, the BMEL-β-cat cell line developed only a few small colonies, while BMEL cells expressing N-myc formed numerous colonies after 4 weeks of plating. Overexpression of both genes did not confer any additional growth advantage to the cells (Figure 4C). These results implicate both β-catenin and Myc in regulating differentiation of murine hepatoblasts, while N-myc displays transforming potential in vitro.

Myc-Induced Liver Tumors Display C2-like HB Phenotype

We sought to address the involvement of Myc signaling in the pathogenesis of human HBs by using a conditional *MYC* transgenic mouse model that develops HB-like tumors (Shachaf et al., 2004; Goga et al., 2007). Histologic analysis of liver tumors from TRE-MYC × LAP-tTA mice showed a hepatoblast-like atypical morphology that is observed in undifferentiated HB (Figure 4D). By qPCR analysis, HB marker genes such as *Dlk1*, *Tacstd1*, and the imprinted genes *Bex1*, *Igf2*, *Meg3*, *Peg3*, and *Peg10* were strongly overexpressed in mouse Myc-induced

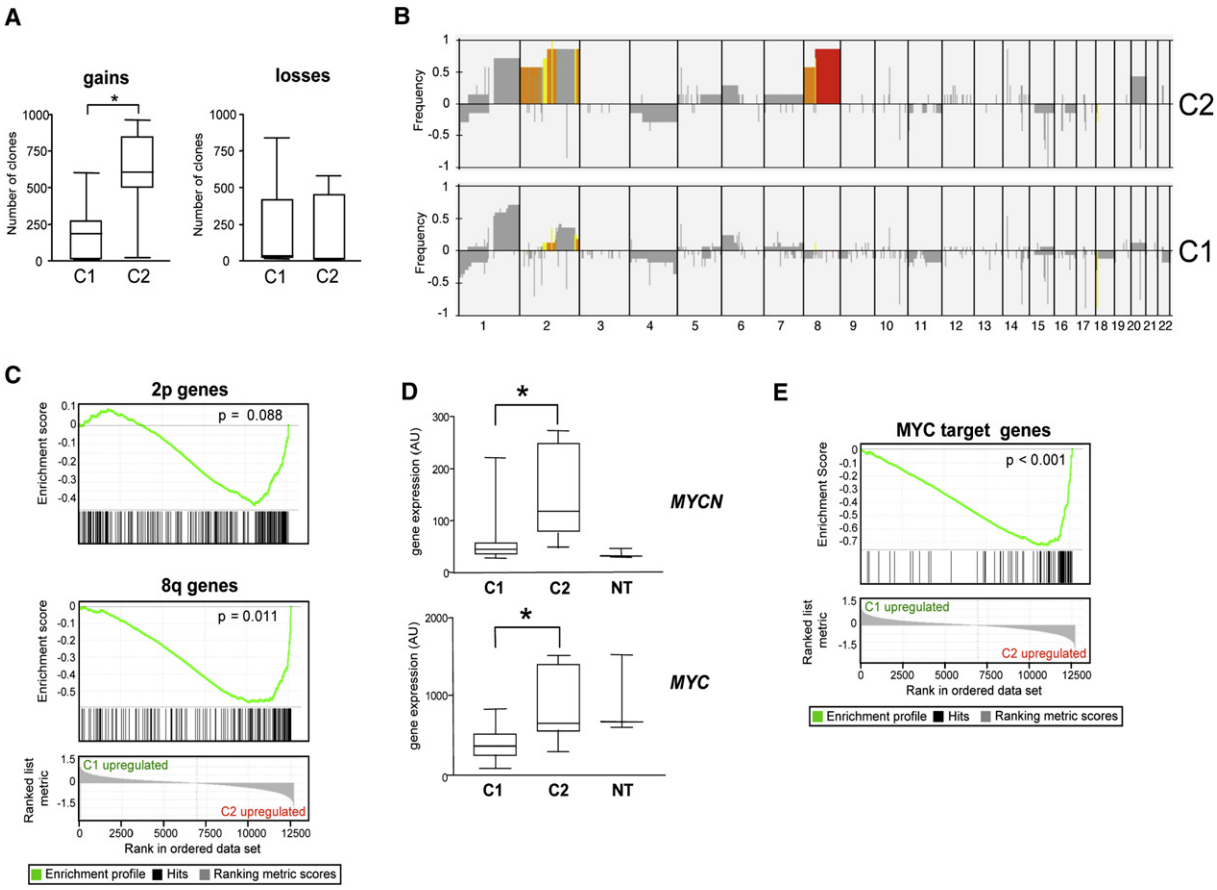

Figure 3. Specific Genetic Profiles of HB Subclasses

(A) Box-plot representation of DNA copy changes in the two HB subclasses. Boxes represent 25–75 percentile range; vertical lines represent 10–90 percentile range; horizontal bars represent median. *p < 0.01.

(B) Chromosome-by-chromosome representation of genomic profiles in HB subclasses C2 (top) and C1 (bottom). For each chromosome, DNA clones were stretched on the x axis along with their position. Genomic alteration frequency is indicated on the y axis (log_2 scale), where positive values correspond to gains and negative values to losses. Significant differences between C1 and C2 were evaluated by Fisher's exact test: red, p < 0.001; orange, p < 0.005; yellow, p < 0.01; gray, no statistical significance.

(C) Gene set enrichment analysis (GSEA) plots using gene sets mapping to chromosomes 2p (gene set S = 227 genes, false discovery rate [FDR] = 0.183) and 8q (gene set S = 169 genes, FDR = 0.051).

(D) Box-plot analysis of *MYCN* and *MYC* expression in C1 and C2 subclasses and in nontumor livers (NT), as in (A). AU, arbitrary units. *p < 0.05.

(E) GSEA plot showing enrichment of upregulated Myc target genes in C2 versus C1 HBs (gene set S = 88 genes, FDR < 0.001) (Zeller et al., 2003).

tumors (Figure S5C). Moreover, similar to human C2 HBs, murine tumors exhibited strong expression of Afp by immunohistochemical analysis, and despite consistent cytoplasmic localization of β-catenin, which indicates Wnt pathway activation, they did not express Glul (Figure 4D). Finally, four Myc-induced tumors were profiled by qPCR with the 16-gene signature. In unsupervised analysis, these tumors coclustered with human rC2 HBs (Figure 4E), and using a class discovery approach, all six algorithms readily classified the murine tumors in the C2 subclass. These data support a primary role of Myc in the pathogenesis of immature human HBs.

Sustained Myc Expression Is Required for Maintaining C2-like Phenotype and Tumorigenic Potential of Established HB Cell Lines

We next evaluated the impact of β-catenin and Myc activation on HB phenotype using RNA interference in Huh6 and HepG2 cell lines derived from pediatric HB or HB/HCC. These cells carry mutant β-catenin alleles and abundantly express c-Myc, showing approximately 30-fold higher expression levels for *MYC* than for *MYCN* by qPCR analysis (data not shown). Given the high functional redundancy of Myc proteins (Malynn et al., 2000), we focused on the effects of c-Myc inhibition. Transfection of Huh6 and HepG2 cells with β-catenin or c-Myc siRNAs resulted in significant decrease of the target proteins compared to cells transfected with nontargeting scrambled control (SC) siRNA (Figure 5A). The β-catenin siRNA more efficiently suppressed wild-type and mutated (G34V) β-catenin in Huh6 cells than the N-terminally deleted protein in HepG2 cells, but strong repression of the Wnt target c-Myc was observed in both cell lines (Figure 5A).

Analysis of the 16-gene signature in Huh6 and HepG2 cells indicated that cells transfected with control siRNA classified as C2 HBs, consistent with high levels of Myc expression (Figure 5B).

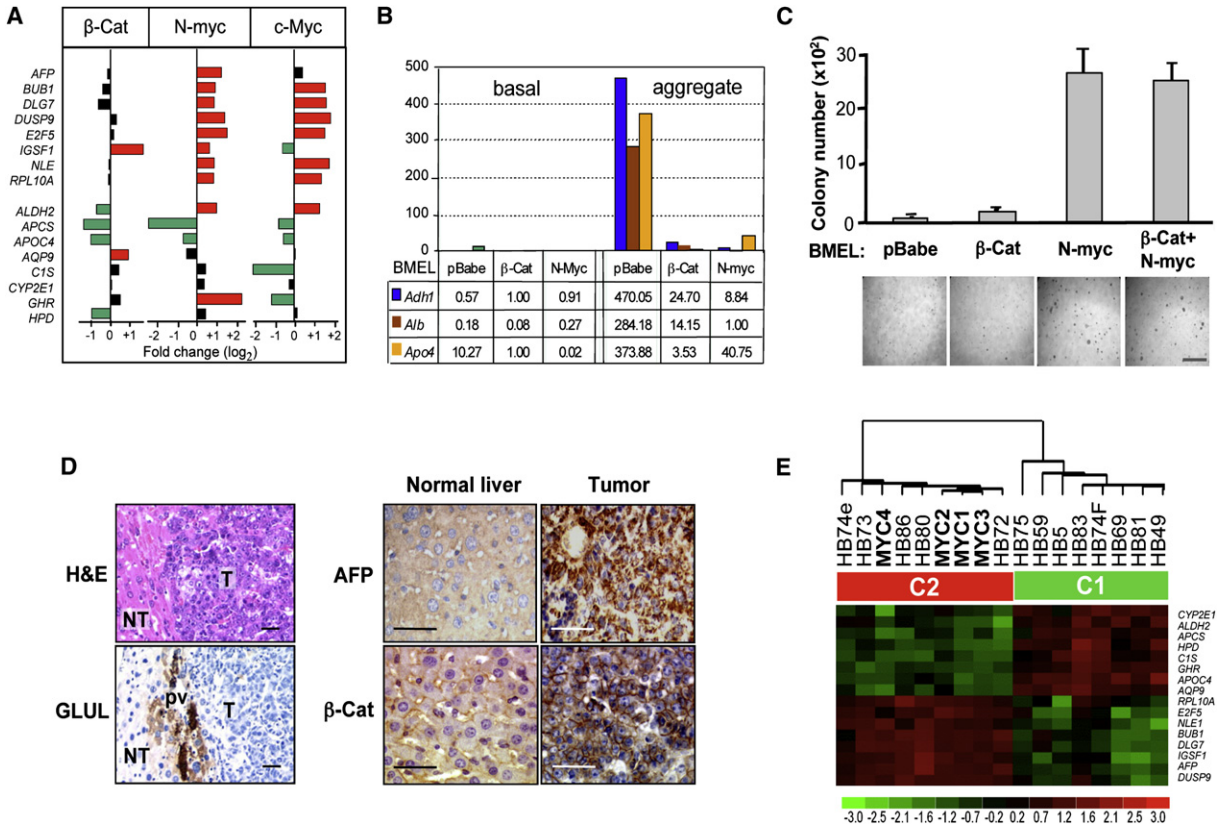

Figure 4. Analysis of Aberrant Activation of β-Catenin or Myc in Murine Hepatoblasts and Myc-Induced Liver Tumor Phenotype

(A) Expression of the 16 genes of the HB classifier in BMEL cells overexpressing β-catenin or Myc genes. Values are expressed as fold change compared with control BMEL cells. Red and green bars indicate high and low expression, respectively. Black bars indicate <0.6-fold log change (1.5-fold in linear scale).

(B) Expression of differentiation markers in BMEL cells stably overexpressing β-catenin or N-myc. BMEL cells transduced with empty pBabe vector were used as control. Data are given as normalized fold-change expression.

(C) Colony formation in soft agar. Error bars = SD; scale bar = 1 mm.

(D) Histology and immunohistochemistry of murine Myc-induced tumors (T) and normal livers (NT). pv, perivenous area. Scale bars = 50 μm.

(E) Unsupervised hierarchical clustering analysis of four murine Myc-induced tumors (MYC1–4) and human rC1 and rC2 HB samples using the 16-gene signature.

Cells transfected with β-catenin or c-Myc siRNA showed a dramatic change in gene expression leading to a C1-like profile. As C2 HBs differ from C1 HBs by high proliferative activity, we measured proliferation of cells transfected with β-catenin, c-Myc, or SC siRNAs. Comparison of proliferation curves showed that proliferation of HepG2 and Huh6 cells was impaired by β-catenin or c-Myc siRNA (Figure 5C). We next compared the effects of β-catenin and Myc on cell tumorigenicity. We have shown recently that inhibition of β-catenin impairs anchorage-independent growth of hepatoma cells in vitro (Renard et al., 2007). We tested the ability of Huh6 and HepG2 cells to form colonies in soft agar after treatment with siRNAs for β-catenin or c-Myc. Consistent with proliferation data, colony formation was reduced by 5- to 8-fold in siβ-catenin- and siMyc-transfected cells at 3 weeks after plating compared to cells transfected with SC siRNA (Figure 5D). To extend our studies to an in vivo setting, Huh6 cells at 48 hr after transfection with siRNA for β-catenin, c-Myc, or SC siRNA were injected subcutaneously into nude mice (n = 4 for each experimental condition). Control siSC-transfected cells formed tumors in mice in less than 3 weeks, while tumors developed after 4 weeks in mice injected with siβ-catenin-transfected cells and after 5 weeks in mice injected with cells transfected with siMyc-transfected cells (Figure 5E). Thus, Myc appears to play a crucial role in the tumorigenicity of HB-derived cells.

The 16-Gene Signature Is a Strong Independent Prognostic Factor

To investigate the clinical relevance of HB molecular classification, the 16-gene HB classifier was assessed in a new set of 77 HB samples from 61 patients by qPCR (Figure 6A; Tables S1, S2, and S11). Extending our previous observation, C1/C2 classification of this new tumor set using the six algorithms was unrelated to *CTNNB1* mutation rate. Using qPCR, we also confirmed enhanced expression of the liver progenitor markers *AFP*, *TACSTD1*, and *KRT19* in C2 tumors (Figure S6). Moreover, while a similar percentage of C1 and C2 tumors displayed mesenchymal components, 95% of C1 tumors showed a predominantly fetal histotype, whereas in 82% of C2 tumors, the major component displayed less differentiated patterns such as embryonal, crowded fetal, and macrotrabecular ($p < 0.0001$) (Table S1). To further assess the association of HB subclasses with liver

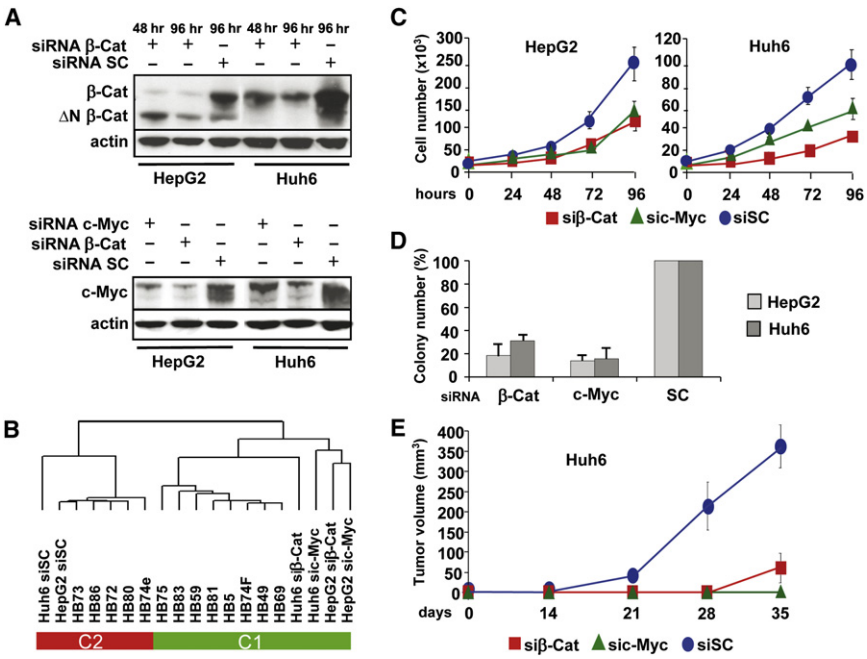

Figure 5. Inhibition of Myc Impairs C2-like Phenotype and Tumorigenicity of HB Cell Lines In Vivo

(A) Immunoblot analysis of β-catenin (upper panel) and c-Myc (lower panel) in HepG2 and Huh6 cells transfected with β-catenin (β-Cat), c-Myc, or scrambled (SC) siRNA. Unless indicated, cell extracts were prepared 96 hr posttransfection. ΔN β-Cat indicates mutated form of β-catenin in HepG2 cells.

(B) Classification of HepG2 and Huh6 cells treated with siRNAs against β-catenin (siβ-Cat), c-Myc (sic-Myc), or nontargeting control (siSC) shown in representative clustering with rC1 and rC2 HB samples.

(C) Cell proliferation in HepG2 and Huh6 cell lines transfected with siβ-Cat, sic-Myc, or siSC. Error bars = SD.

(D) Soft-agar assay. HepG2 and Huh6 cells were transfected with siRNAs specifically targeting β-catenin, c-Myc, or nontargeting control (SC) as indicated. Colony number is expressed as percentage of colonies in siSC-transfected cells. Error bars = SD.

(E) In vivo tumorigenesis assays. Data are presented as mean tumor volume ± SD.

development, five human fetal livers at different weeks of gestation were included in the qPCR studies. Fetal livers at late (>35 weeks) and earlier (17–26 weeks) developmental stages were classified as C1 and C2, respectively, further supporting that HB subclasses reflect different developmental phases (Figure 6A).

The clinical impact of HB molecular classification was addressed in the complete set of patients, comprising 54 C1 (63%) and 31 C2 (36%) cases. Besides strong association with predominantly immature histotypes, C2 HBs were tightly associated with features of advanced tumor stage, such as vascular invasion and extrahepatic metastasis (Figure 6B). Accordingly, overall survival of these patients was markedly impaired. Kaplan-Meier estimates of overall survival probability at 2 years were 44% for patients with C2 tumors and 92% for patients with C1 tumors ($p < 0.0001$), and similar trends were seen for disease-free survival (data not shown). The observation of higher numbers of C2-type cases in diagnostic biopsies compared to posttreatment specimens prompted us to examine whether preoperative chemotherapy treatment could affect tumor classification. We compared the 16-gene expression profiles between untreated and treated samples by t test and found no significant difference. We then examined the performance of the 16-gene signature in untreated and treated samples. Analysis of the 73 samples resected after chemotherapy showed a significant difference in outcome between patients with C1 and C2 HBs ($p = 0.0001$) (Figure 6C). Remarkably, Kaplan-Meier analysis also confirmed the C2 subclass as a poor prognostic group in 28 cases for which biopsies or surgery specimens before chemotherapy were available ($p = 0.0283$) (Figure 6C). Thus, increased frequency of C2 subtypes in untreated versus posttreatment samples is likely related to clinical practice, as diagnostic biopsies are prescribed mostly for clinically unfavorable cases. Collectively, these data strongly suggest that chemotherapy does not significantly modify the expression profiles used for molecular classification of HB. Of note, available pretreatment biopsies were assigned to the same subclass as matched resected tumors in 14 out of 16 cases (see Figure 6A; Table S2).

We further assessed the prognostic validity of the 16-gene signature for all patients in multivariate analysis, using a Cox proportional hazards model with pathological and clinical variables associated with patients' survival. This analysis identified the signature as an independent prognostic factor, with better performance than tumor stage defined by pretreatment extent of disease (PRETEXT), vascular invasion, and extrahepatic metastases (Figure 6B). Thus, this signature demonstrates strong prognostic relevance when compared to current clinical criteria.

DISCUSSION

In this paper, integrated molecular and genetic studies of hepatoblastoma disclosed two major molecular subclasses of tumors that evoke early and late phases of prenatal liver development. Major differences in expression profiles of the two HB subtypes led us to elucidate a 16-gene signature that proved highly efficient in stratifying HBs as well as normal livers according to hepatic developmental stage. Using this signature, we could establish a tight correlation between stage of hepatic differentiation and clinical behavior, notably vascular invasion, metastatic spread, and patient survival (Figure 7). Aberrant activation of the Wnt pathway represents a seminal event in both tumor types, with cumulated mutation rates of β-catenin, APC, and AXIN over 80%. Additionally, the interplay of Wnt/β-catenin and Myc signaling in immature tumors activates a distinct transcriptional program that correlates with tumor aggressiveness.

HB Molecular Subclasses Are Determined by Liver Differentiation Stages

Here we present a robust methodological approach for molecular classification that relies entirely on tumor transcriptional profiling, independently of sample-associated genetic, histologic, and

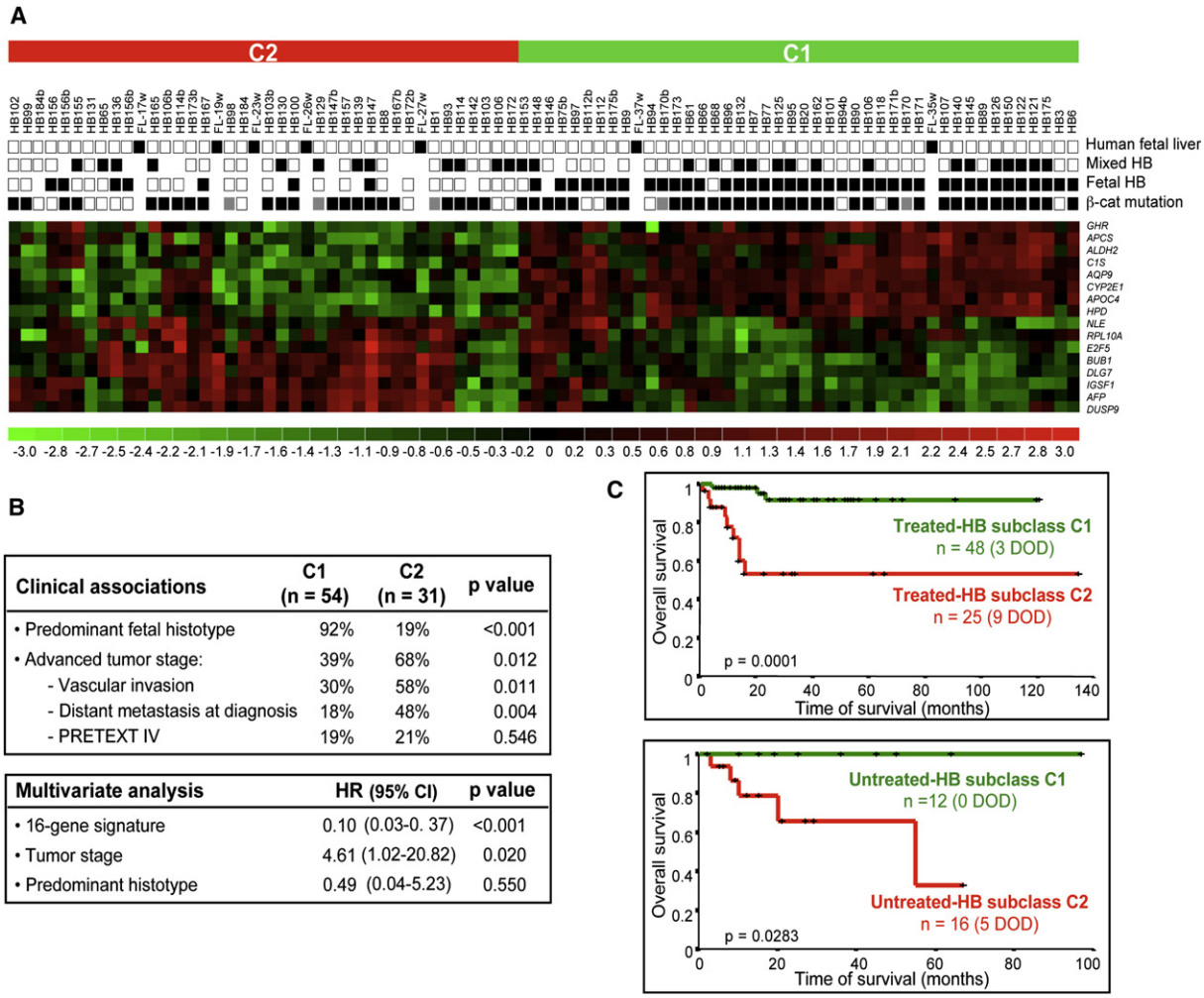

Clinical associations	C1 (n = 54)	C2 (n = 31)	p value
• Predominant fetal histotype	92%	19%	<0.001
• Advanced tumor stage:	39%	68%	0.012
- Vascular invasion	30%	58%	0.011
- Distant metastasis at diagnosis	18%	48%	0.004
- PRETEXT IV	19%	21%	0.546

Multivariate analysis	HR (95% CI)	p value
• 16-gene signature	0.10 (0.03-0. 37)	<0.001
• Tumor stage	4.61 (1.02-20.82)	0.020
• Predominant histotype	0.49 (0.04-5.23)	0.550

Figure 6. Molecular Classification Using the 16-Gene Signature Correlates with Clinical Behavior

(A) Expression profiles of the 16 genes forming the HB classifier are shown as a heat map indicating high (red) and low (green) expression according to a $\log_2$-transformed scale. HBs and human fetal livers (FL) at different weeks (w) of gestation were assigned to class 1 or 2 using the 16-gene expression profile. Black boxes in the rows above the heat map indicate (from top to bottom) human fetal liver, mixed epithelial-mesenchymal histology, predominantly fetal histotype, and β-catenin mutation. Gray boxes indicate familial adenomatous polyposis (FAP) cases.

(B) Top: association of clinical and pathological data with HB classification (chi-square test). Pretreatment extent of disease (PRETEXT) IV stage indicates tumor involvement of all liver sections. Bottom: multivariate analysis including three variables associated with patient survival. The predominant histotype is defined as either fetal or nonfetal (including embryonal, crowded fetal, or macrotrabecular types). Tumor stage is defined by vascular invasion, distant metastasis at diagnosis, and PRETEXT stage. HR, hazard ratio; CI, confidence interval.

(C) Top: Kaplan-Meier plots of overall survival for 73 patients that received preoperative chemotherapy. Bottom: overall survival of 28 HB patients for which pretreatment biopsies or primary surgery specimens from untreated patients were available.

clinical annotations. In the absence of predefined class labels, this approach does not fulfill classical criteria of predictive analysis, and validation of the classifier efficacy was provided by strong association of each subclass with identical clinical and pathological parameters in two different tumor sets.

The most significant difference between HB subclasses can be ascribed to distinct hepatic differentiation stages, as defined by comparison with mouse livers at various embryonic stages and by morphological patterns. The C1 subclass recapitulates liver features at late stages of intrauterine life, with an expression profile similar to murine livers at E14.5–E18.5 and a mostly fetal histotype, while the C2 subclass resemble earlier stages of liver development, with a transcriptional program evoking murine livers at E11.5–E12.5 and a predominantly embryonal histotype. These results are in line with recent studies using cross-species comparisons. Clinically distinct medulloblastoma subtypes have been identified by their similarity with precise stages of murine cerebellar development (Kho et al., 2004). Similarly, Wilms' tumor shares expression of stemness and imprinted genes with murine metanephric blastema (Dekel et al., 2006). A salient feature of immature HBs is the characteristic interplay of stemness and high proliferation found in aggressive tumors (Glinsky et al., 2005). The C2 expression profile is significantly enriched in markers of hepatic progenitor cells such as cytokeratin 19 and Ep-CAM (Roskams, 2006), as well as in mitotic cell-cycle and spindle assembly checkpoint regulators, including cyclin B1,

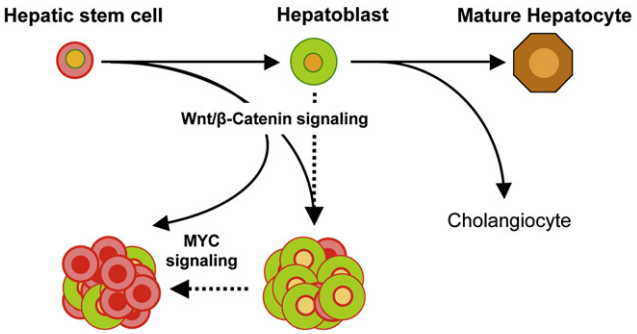

C2-type HB	C1-type HB	Features
24/31 (77%)	46/54 (85%)	· Wnt pathway-related mutations
Proliferation and antiapoptotic genes	Liver perivenous genes	· Overexpressed β-catenin targets
AFP +++ Ep-CAM +++ KRT19 +	AFP + Ep-CAM + KRT19 -	· Hepatic progenitor markers
Early fetal	Late fetal/postnatal	· Liver developmental stage
High	Low	· Proliferation rate
Cell cycle, mitotic checkpoint, Myc signaling	Hepatic perivenous metabolism	· Gene signatures (GO, KEGG and GSEA)
High	Low	· Chromosomal instability
+2p, +8q	-	· Specific chromosomal changes
Embryonal, Crowded fetal, Macrotrabecular	Fetal, pure fetal	· Histological main component
Advanced	Early	· Tumor stage
Unfavorable	Favorable	· Disease outcome

Figure 7. Summary of Biological and Clinical Characteristics of HB Subclasses

Steps of normal liver development are shown at the top. HB might arise from impairment of the normal liver differentiation program associated with excessive Wnt/β-catenin signaling. Activation of Myc signaling that characterizes the aggressive tumor phenotype might depend on genetic alterations or tumor differentiation stage. The table below lists major distinctive features of the two HB subtypes.

BUB1, BUB1B, and Aurora kinases. Overexpression of these kinases or other components of the spindle checkpoint induces centrosome amplification and defects in chromosome segregation leading to chromosome number instability and aneuploidy (Marumoto et al., 2005).

Context-Dependent Transcriptional Programs Driven by Wnt Signaling

Mutational activation of β-catenin is a hallmark of HB, and accordingly, intracellular accumulation of the protein was observed in virtually all tumors, albeit with variable frequencies and intensities. Both immature and differentiated tumors overexpressed *AXIN2* and *DKK1*, in an attempt to activate a negative feedback loop aimed at limiting the Wnt signal. However, the two HB subtypes showed significant differences in β-catenin immunoexpression, with nuclear accumulation and decreased membranous localization of the protein in poorly differentiated tumors. Heterogeneous distribution of nuclear β-catenin within colorectal tumors has been linked to different levels of Wnt signaling activity resulting from differential combinations of autocrine and paracrine factors (Fodde and Brabletz, 2007). In immature HBs, nuclear β-catenin might be related to the absence of membranous E-cadherin, as we have reported previously (Wei et al., 2000), and/or to cross-talk with growth-stimulating pathways evidenced in less differentiated cells (Wu et al., 2008).

The differential expression of hepatic Wnt targets in HB subtypes raises the possibility of context-dependent activation of Wnt target genes. In the liver, Wnt/β-catenin signaling is known to govern metabolic zonation by positively controlling the perivenous gene expression program and negatively controlling the periportal program (Benhamouche et al., 2006). In C1 HBs, hepatic perivenous markers such as *GLUL* were overexpressed and genes encoding periportal functions such as *GLS2* were downregulated, while the zonation-related profile was lessened in C2 HBs. This might reflect the cooperation of β-catenin/Tcf with liver-enriched factors that are downregulated in immature tumors. Moreover, cell-type-specific regulation of Wnt targets might comprise multilayered control systems involving distinct promoter occupancy by TCFs and epigenetic factors (Merrill et al., 2001; Wohrle et al., 2007).

Genetic Instability in Poorly Differentiated Tumors

The profile of genetic aberrations determined here by aCGH revealed a limited number of chromosomal imbalances in HB, in general agreement with previous karyotyping and CGH studies (Tomlinson et al., 2005; Weber et al., 2000). Gains on chromosomes 8q and 20 in HB have been associated with poor outcome (Weber et al., 2000). However, relationships between genetic defects and HB histotypes have not been addressed so far. By integrating genetic data with expression profiling, we have provided evidence for a strong association of immature and aggressive HBs with chromosomal instability. This trait was manifested by increased DNA copy gains, particularly on chromosomes 2 and 8, and to a minor extent on chromosome 20. These alterations likely influence tumor phenotype, as *E2F5* (chromosome 8q21) and *BUB1* (chromosome 2q14) belong to the 16-gene HB classifier. Among candidate genes on chromosomes 2p and 8q that could play a role in the aggressive HB phenotype, *MYCN* and *MYC* are frequently overexpressed in human cancer and are associated with poor prognosis (Vita and Henriksson, 2006).

Influence of Myc Activation on Proliferation, Differentiation, and Tumorigenesis in Hepatic Model Systems

Our studies provided evidence for a drastic role of Myc deregulation in different experimental systems. When overexpressed in murine hepatoblasts, N-myc induced a shift from C1-like type to C2-like type. However, N-myc alone or in association with β-catenin failed to confer tumorigenic properties to BMEL cells in immunocompromised mice (unpublished data). This might be related to the wild-type p53 background in these cells, as suggested by previous work (Zender et al., 2005). Conversely, inhibition of β-catenin or c-Myc in established hepatoblastoma cell lines converted the C2-like phenotype to a milder, C1-like profile. Impaired tumorigenesis conferred by Myc repression in cells with constitutively activated β-catenin argues for a role of Myc genes as main effectors of the oncogenic Wnt/β-catenin pathway in aggressive HBs.

Myc is among the most potent oncogenes associated with HCC development in mice (Vita and Henriksson, 2006). Our finding that mouse liver tumors induced by c-Myc resemble immature human HBs suggests that the 16-gene signature enables the identification of Myc activation in liver tumors and might represent a valuable tool to stratify patients amenable for direct or indirect therapeutic targeting of Myc (Goga et al., 2007; Vita and Henriksson, 2006).

Clinical Implications

The correlation between clinical behavior and differentiation/proliferation status observed in HB is common to many human solid tumors. In our study, this correlation was mainly determined by differences in tumor invasive properties, clinical tumor stage, and patient outcome. Most importantly, we have shown that the 16-gene HB classifier discriminates aggressive tumors, exhibits powerful survival predictor capacities, and demonstrates strong prognostic relevance when compared to clinical criteria in multivariate analysis. In current clinical practice, frequent cellular heterogeneity in HBs has hampered the use of histopathologic criteria as a prognostic tool. The expression signature afforded here enables direct appraisal of the global degree of tumor cell maturation, allowing the bypass of these difficulties. Moreover, the signature shows equal prognostic capacity when applied to diagnostic biopsies or posttreatment resected tumors, and when assayed on paired samples, it assigns almost 90% of biopsies and matched treated samples to the same category. Further studies in larger series are needed to warrant the use of a clinical tool based on the molecular signature to improve the outcome prediction and clinical management of HB.

In light of recent evidence showing that HCC subtypes with poor prognosis may arise from hepatic progenitor cells (Lee et al., 2006; Roskams, 2006; Yamashita et al., 2008), it would be worth examining the value of the genomic signature described herein for classification of common adult liver tumors. Moreover, the present study offers an opportunity to identify therapies matching the mechanisms that lead to malignant transformation of liver progenitor cells.

EXPERIMENTAL PROCEDURES

Patients and Tissue Samples

A total of 102 tumor specimens and biopsies from 85 patients with HB were collected from different hospitals in France (77 cases), Italy (6 cases), the UK (1 case), and Switzerland (1 case). Seventy-three patients received chemotherapy treatment prior to surgery, most being enrolled in clinical trials of the International Childhood Liver Tumour Strategy Group (SIOPEL) (Perilongo et al., 2000). Tumor and liver samples were snap frozen and stored at −80°C. Tables S1 and S2 describe patient characteristics and clinicopathological parameters. Histology of all tumor specimens was centrally reviewed by an expert pathologist (M.F.). The study was approved by the Biomedical Research Committee of Institut Pasteur, and informed consent was obtained at each medical center in accordance with European Union guidelines for biomedical research.

Gene Mutation Analysis

CTNNB1 mutational screening was performed as described previously (Wei et al., 2000). Primer sequences and PCR protocol for *AXIN1* and *AXIN2* mutation screening are described in Supplemental Experimental Procedures.

Oligonucleotide Microarrays

25 HB samples and 4 nontumor samples were selected for Affymetrix HG-U133A oligonucleotide array analysis based on RNA quality (28S/18S ratio > 1.5, RIN [RNA integrity number] > 8; Agilent 2100 Bioanalyzer), complete clinical annotations, expert pathological review, and representative coverage of clinicopathological situations. Total RNA was prepared using the FastPrep system (Qbiogene) and an RNeasy Mini Kit (QIAGEN). E18.5 mouse fetal livers and postnatal livers at 8 days after birth were profiled on Affymetrix MG-U74A and B v2 arrays according to the manufacturer's instructions. Data analysis is described in detail in Supplemental Experimental Procedures.

Array-Based Comparative Genomic Hybridization

Genomic DNA from 24 HBs and 3 nontumor samples was analyzed on chips containing 3400 sequence-verified PAC/BAC clones spaced at approximately 1 Mb intervals. Array CGH protocol and data analysis are described in Supplemental Experimental Procedures.

Quantitative PCR Analysis

Total RNA was extracted from human and murine liver tissues and cell lines (28S/18S ratio > 1.0, RIN > 7), and human fetal liver RNAs were purchased from BioChain Institute, Inc. cDNA was generated by using SuperScript II reverse transcriptase (Invitrogen) with random primers (Promega) according to the manufacturer's protocol. For qPCR, we used Sybr Green Master Mix (Applied Biosystems) and an ABI PRISM 7900HT instrument. Reference genes were chosen as described in Supplemental Experimental Procedures.

Cell Culture, Transfection, and Soft-Agar Assays

Cell lines, transfection protocols, and proliferation and soft-agar assays are described in Supplemental Experimental Procedures.

Myc-Driven Liver Tumor Model

Myc-driven liver tumors were generated as described previously (Goga et al., 2007). Briefly, TRE-MYC mice were crossed to LAP-tTA (liver-specific promoter) mice. Animals were maintained on doxycycline (200 mg/kg doxy chow) to suppress MYC expression until 8 weeks of age. Doxycycline was then removed, and mice were followed for evidence of tumor formation. All experiments were approved by the Committee on Animal Research at UCSF.

Human Xenografts

Female athymic *nu/nu* Balb/c mice (8 weeks of age, Charles River Laboratories) were inoculated subcutaneously with 5×10^6 Huh6 cells in 1 ml PBS. Tumor volume (v) was determined in mm^3 by measuring the tumor length (l) and width (w) and calculated using the formula: $v = lw^2/2$. Tumors were fixed and sectioned for histologic analysis. All procedures were performed according to protocols approved by the Animal Facility veterinarian board of Institut Pasteur.

Western Blotting and Immunohistochemistry

Protocols and antibodies are described in Supplemental Experimental Procedures.

Clinical Data Analysis

We used the chi-square test for comparisons between groups. Survival curves were calculated using the Kaplan-Meier method and the log-rank test. Variables independently related to survival were determined by stepwise forward Cox regression analysis.

ACCESSION NUMBERS

Microarray data described herein are available at ArrayExpress (http://www.ebi.ac.uk/microarray-as/ae/) under the accession numbers E-MEXP-1851 (HB transcriptome), E-MEXP-1852 (HB aCGH), and E-MEXP-1853 (mouse liver).

SUPPLEMENTAL DATA

The Supplemental Data include Supplemental Experimental Procedures, Supplemental References, six figures, and seventeen tables and can be found with this article online at http://www.cancercell.org/supplemental/S1535-6108(08)00369-3.

ACKNOWLEDGMENTS

We thank D. Geromin and J.Y. Coppée for RNA and DNA qualification; C. Thibault for hybridization of oligonucleotide microarrays; P.Y. Cousin, E. Manié, and O. Delattre for hybridization of CGH arrays; L. Ma and C. Bouchier for genomic DNA sequencing; and M.J. Redon for immunohistochemical analysis. We also thank B. Majello, J. Nevins, and C. Missero for expression vectors and P. Czauderna, G. Perilongo, D. Pariente, and clinicians involved in SIOPEL studies for help with referring patients.

This work was supported by the "Carte d'Identité des Tumeurs" program of the Ligue Nationale Contre le Cancer. A.G. was supported by grant IRG-97-150-10 from the American Cancer Society and the Sandler Family Program in Biological Sciences. S.C. was supported by the GIS-Institut des Maladies Rares and the Fondation pour la Recherche Médicale. C.A. was supported by an EASL Sheila Sherlock Fellowship and the Fondation pour la Recherche Médicale.

Received: November 13, 2007
Revised: August 13, 2008
Accepted: November 3, 2008
Published: December 8, 2008

REFERENCES

Assou, S., Le Carrour, T., Tondeur, S., Strom, S., Gabelle, A., Marty, S., Nadal, L., Pantesco, V., Reme, T., Hugnot, J.P., et al. (2007). A meta-analysis of human embryonic stem cells transcriptome integrated into a web-based expression atlas. Stem Cells *25*, 961–973.

Benhamouche, S., Decaens, T., Godard, C., Chambrey, R., Rickman, D.S., Moinard, C., Vasseur-Cognet, M., Kuo, C.J., Kahn, A., Perret, C., and Colnot, S. (2006). Apc tumor suppressor gene is the "zonation-keeper" of mouse liver. Dev. Cell *10*, 759–770.

Boyault, S., Rickman, D.S., de Reynies, A., Balabaud, C., Rebouissou, S., Jeannot, E., Herault, A., Saric, J., Belghiti, J., Franco, D., et al. (2007). Transcriptome classification of HCC is related to gene alterations and to new therapeutic targets. Hepatology *45*, 42–52.

Braeuning, A., Ittrich, C., Kohle, C., Hailfinger, S., Bonin, M., Buchmann, A., and Schwarz, M. (2006). Differential gene expression in periportal and perivenous mouse hepatocytes. FEBS J. *273*, 5051–5061.

Cadoret, A., Ovejero, C., Terris, B., Souil, E., Levy, L., Lamers, W.H., Kitajewski, J., Kahn, A., and Perret, C. (2002). New targets of beta-catenin signaling in the liver are involved in glutamine metabolism. Oncogene *21*, 8293–8301.

Capurro, M.I., Xiang, Y.Y., Lobe, C., and Filmus, J. (2005). Glypican-3 promotes the growth of hepatocellular carcinoma by stimulating canonical Wnt signaling. Cancer Res. *65*, 6245–6254.

Cavard, C., Terris, B., Grimber, G., Christa, L., Bussiere, B., Simon, M.T., Renard, C.A., Buendia, M.A., and Perret, C. (2006). Overexpression of regenerating islet-derived 1 alpha and 3 alpha genes in human primary liver tumors with beta-catenin mutations. Oncogene *25*, 599–608.

Dekel, B., Metsuyanim, S., Schmidt-Ott, K.M., Fridman, E., Jacob-Hirsch, J., Simon, A., Pinthus, J., Mor, Y., Barasch, J., Amariglio, N., et al. (2006). Multiple imprinted and stemness genes provide a link between normal and tumor progenitor cells of the developing human kidney. Cancer Res. *66*, 6040–6049.

de La Coste, A., Romagnolo, B., Billuart, P., Renard, C.A., Buendia, M.A., Soubrane, O., Fabre, M., Chelly, J., Beldjord, C., Kahn, A., and Perret, C. (1998). Somatic mutations of the beta-catenin gene are frequent in mouse and human hepatocellular carcinomas. Proc. Natl. Acad. Sci. USA *95*, 8847–8851.

Fodde, R., and Brabletz, T. (2007). Wnt/beta-catenin signaling in cancer stemness and malignant behavior. Curr. Opin. Cell Biol. *19*, 150–158.

Glinsky, G.V., Berezovska, O., and Glinskii, A.B. (2005). Microarray analysis identifies a death-from-cancer signature predicting therapy failure in patients with multiple types of cancer. J. Clin. Invest. *115*, 1503–1521.

Goga, A., Yang, D., Tward, A.D., Morgan, D.O., and Bishop, J.M. (2007). Inhibition of CDK1 as a potential therapy for tumors over-expressing MYC. Nat. Med. *13*, 820–827.

Ishak, K.G., and Glunz, P.R. (1967). Hepatoblastoma and hepatocarcinoma in infancy and childhood: report of 47 cases. Cancer *20*, 396–422.

Kho, A.T., Zhao, Q., Cai, Z., Butte, A.J., Kim, J.Y., Pomeroy, S.L., Rowitch, D.H., and Kohane, I.S. (2004). Conserved mechanisms across development and tumorigenesis revealed by a mouse development perspective of human cancers. Genes Dev. *18*, 629–640.

Kirmizis, A., Bartley, S.M., and Farnham, P.J. (2003). Identification of the polycomb group protein SU(Z)12 as a potential molecular target for human cancer therapy. Mol. Cancer Ther. *2*, 113–121.

Koch, A., Denkhaus, D., Albrecht, S., Leuschner, I., von Schweinitz, D., and Pietsch, T. (1999). Childhood hepatoblastomas frequently carry a mutated degradation targeting box of the β-catenin gene. Cancer Res. *59*, 269–273.

Koch, A., Waha, A., Hartmann, W., Hrychyk, A., Schuller, U., Wharton, K.A., Jr., Fuchs, S.Y., Schweinitz, D., and Pietsch, T. (2005). Elevated expression of wnt antagonists is a common event in hepatoblastomas. Clin. Cancer Res. *11*, 4295–4304.

Korinek, V., Barker, N., Moerer, P., van Donselaar, E., Huls, G., Peters, P.J., and Clevers, H. (1998). Depletion of epithelial stem-cell compartments in the small intestine of mice lacking Tcf-4. Nat. Genet. *19*, 379–383.

Lee, J.S., Heo, J., Libbrecht, L., Chu, I.S., Kaposi-Novak, P., Calvisi, D.F., Mikaelyan, A., Roberts, L.R., Demetris, A.J., Sun, Z., et al. (2006). A novel prognostic subtype of human hepatocellular carcinoma derived from hepatic progenitor cells. Nat. Med. *12*, 410–416.

Lowry, W.E., Blanpain, C., Nowak, J.A., Guasch, G., Lewis, L., and Fuchs, E. (2005). Defining the impact of beta-catenin/Tcf transactivation on epithelial stem cells. Genes Dev. *19*, 1596–1611.

Ma, S., Chan, K.W., Hu, L., Lee, T.K., Wo, J.Y., Ng, I.O., Zheng, B.J., and Guan, X.Y. (2007). Identification and characterization of tumorigenic liver cancer stem/progenitor cells. Gastroenterology *132*, 2542–2556.

Malynn, B.A., de Alboran, I.M., O'Hagan, R.C., Bronson, R., Davidson, L., DePinho, R.A., and Alt, F.W. (2000). N-myc can functionally replace c-myc in murine development, cellular growth, and differentiation. Genes Dev. *14*, 1390–1399.

Marumoto, T., Zhang, D., and Saya, H. (2005). Aurora-A - a guardian of poles. Nat. Rev. Cancer *5*, 42–50.

McLin, V.A., Rankin, S.A., and Zorn, A.M. (2007). Repression of Wnt/beta-catenin signaling in the anterior endoderm is essential for liver and pancreas development. Development *134*, 2207–2217.

Merrill, B.J., Gat, U., DasGupta, R., and Fuchs, E. (2001). Tcf3 and Lef1 regulate lineage differentiation of multipotent stem cells in skin. Genes Dev. *15*, 1688–1705.

Micsenyi, A., Tan, X., Sneddon, T., Luo, J.H., Michalopoulos, G.K., and Monga, S.P. (2004). Beta-catenin is temporally regulated during normal liver development. Gastroenterology *126*, 1134–1146.

Ober, E.A., Verkade, H., Field, H.A., and Stainier, D.Y. (2006). Mesodermal Wnt2b signalling positively regulates liver specification. Nature *442*, 688–691.

Ortega, J.A., Douglass, E.C., Feusner, J.H., Reynolds, M., Quinn, J.J., Finegold, M.J., Haas, J.E., King, D.R., Liu-Mares, W., Sensel, M.G., and Krailo, M.D. (2000). Randomized comparison of cisplatin/vincristine/fluorouracil and cisplatin/continuous infusion doxorubicin for treatment of pediatric hepatoblastoma: A report from the Children's Cancer Group and the Pediatric Oncology Group. J. Clin. Oncol. *18*, 2665–2675.

Otu, H.H., Naxerova, K., Ho, K., Can, H., Nesbitt, N., Libermann, T.A., and Karp, S.J. (2007). Restoration of liver mass after injury requires proliferative and not embryonic transcriptional patterns. J. Biol. Chem. *282*, 11197–11204.

Perilongo, G., Shafford, E., and Plaschkes, J. (2000). SIOPEL trials using preoperative chemotherapy in hepatoblastoma. Lancet Oncol. *1*, 94–100.

Renard, C.A., Labalette, C., Armengol, C., Cougot, D., Wei, Y., Cairo, S., Pineau, P., Neuveut, C., de Reynies, A., Dejean, A., et al. (2007). Tbx3 is a downstream target of the Wnt/β-catenin pathway and a critical mediator of β-catenin survival functions in liver cancer. Cancer Res. *67*, 901–910.

Reya, T., Morrison, S.J., Clarke, M.F., and Weissman, I.L. (2001). Stem cells, cancer, and cancer stem cells. Nature *414*, 105–111.

Roskams, T. (2006). Liver stem cells and their implication in hepatocellular and cholangiocarcinoma. Oncogene *25*, 3818–3822.

Schnater, J.M., Kohler, S.E., Lamers, W.H., von Schweinitz, D., and Aronson, D.C. (2003). Where do we stand with hepatoblastoma? A review. Cancer *98*, 668–678.

Sekiya, T., Adachi, S., Kohu, K., Yamada, T., Higuchi, O., Furukawa, Y., Nakamura, Y., Nakamura, T., Tashiro, K., Kuhara, S., et al. (2004). Identification of BMP and activin membrane-bound inhibitor (BAMBI), an inhibitor of transforming growth factor-beta signaling, as a target of the beta-catenin pathway in colorectal tumor cells. J. Biol. Chem. *279*, 6840–6846.

Shachaf, C.M., Kopelman, A.M., Arvanitis, C., Karlsson, A., Beer, S., Mandl, S., Bachmann, M.H., Borowsky, A.D., Ruebner, B., Cardiff, R.D., et al. (2004). MYC inactivation uncovers pluripotent differentiation and tumour dormancy in hepatocellular cancer. Nature *431*, 1112–1117.

Stahl, S., Ittrich, C., Marx-Stoelting, P., Kohle, C., Altug-Teber, O., Riess, O., Bonin, M., Jobst, J., Kaiser, S., Buchmann, A., and Schwarz, M. (2005). Genotype-phenotype relationships in hepatocellular tumors from mice and man. Hepatology *42*, 353–361.

Strick-Marchand, H., and Weiss, M.C. (2002). Inducible differentiation and morphogenesis of bipotential liver cell lines from wild-type mouse embryos. Hepatology *36*, 794–804.

Subramanian, A., Tamayo, P., Mootha, V.K., Mukherjee, S., Ebert, B.L., Gillette, M.A., Paulovich, A., Pomeroy, S.L., Golub, T.R., Lander, E.S., and Mesirov, J.P. (2005). Gene set enrichment analysis: a knowledge-based approach for interpreting genome-wide expression profiles. Proc. Natl. Acad. Sci. USA *102*, 15545–15550.

Taniguchi, K., Roberts, L.R., Aderca, I.N., Dong, X., Qian, C., Murphy, L.M., Nagorney, D.M., Burgart, L.J., Roche, P.C., Smith, D.I., et al. (2002). Mutational spectrum of beta-catenin, AXIN1, and AXIN2 in hepatocellular carcinomas and hepatoblastomas. Oncogene *21*, 4863–4871.

Tomlinson, G.E., Douglass, E.C., Pollock, B.H., Finegold, M.J., and Schneider, N.R. (2005). Cytogenetic evaluation of a large series of hepatoblastomas: numerical abnormalities with recurring aberrations involving 1q12-q21. Genes Chromosomes Cancer *44*, 177–184.

Vita, M., and Henriksson, M. (2006). The Myc oncoprotein as a therapeutic target for human cancer. Semin. Cancer Biol. *16*, 318–330.

Weber, R.G., Pietsch, T., von Schweinitz, D., and Lichter, P. (2000). Characterization of genomic alterations in hepatoblastomas. A role for gains on chromosomes 8q and 20 as predictors of poor outcome. Am. J. Pathol. *157*, 571–578.

Wei, Y., Fabre, M., Branchereau, S., Gauthier, F., Perilongo, G., and Buendia, M.A. (2000). Activation of beta-catenin in epithelial and mesenchymal hepatoblastomas. Oncogene *19*, 498–504.

Weinberg, A.G., and Finegold, M.J. (1983). Primary hepatic tumors of childhood. Hum. Pathol. *14*, 512–537.

Wohrle, S., Wallmen, B., and Hecht, A. (2007). Differential control of Wnt target genes involves epigenetic mechanisms and selective promoter occupancy by T-cell factors. Mol. Cell. Biol. *27*, 8164–8177.

Wu, X., Tu, X., Joeng, K.S., Hilton, M.J., Williams, D.A., and Long, F. (2008). Rac1 activation controls nuclear localization of beta-catenin during canonical Wnt signaling. Cell *133*, 340–353.

Yamashita, T., Budhu, A., Forgues, M., and Wang, X.W. (2007). Activation of hepatic stem cell marker EpCAM by Wnt-beta-catenin signaling in hepatocellular carcinoma. Cancer Res. *67*, 10831–10839.

Yamashita, T., Forgues, M., Wang, W., Kim, J.W., Ye, Q., Jia, H., Budhu, A., Zanetti, K.A., Chen, Y., Qin, L.X., et al. (2008). EpCAM and alpha-fetoprotein expression defines novel prognostic subtypes of hepatocellular carcinoma. Cancer Res. *68*, 1451–1461.

Yang, Z.F., Ngai, P., Ho, D.W., Yu, W.C., Ng, M.N., Lau, C.K., Li, M.L., Tam, K.H., Lam, C.T., Poon, R.T., and Fan, S.T. (2008). Identification of local and circulating cancer stem cells in human liver cancer. Hepatology *47*, 919–928.

Yue, W., Sun, Q., Dacic, S., Landreneau, R.J., Siegfried, J.M., Yu, J., and Zhang, L. (2008). Downregulation of Dkk3 activates beta-catenin/TCF-4 signaling in lung cancer. Carcinogenesis *29*, 84–92.

Zeller, K.I., Jegga, A.G., Aronow, B.J., O'Donnell, K.A., and Dang, C.V. (2003). An integrated database of genes responsive to the Myc oncogenic transcription factor: identification of direct genomic targets. Genome Biol. *4*, R69.

Zender, L., Xue, W., Cordon-Cardo, C., Hannon, G.J., Lucito, R., Powers, S., Flemming, P., Spector, M.S., and Lowe, S.W. (2005). Generation and analysis of genetically defined liver carcinomas derived from bipotential liver progenitors. Cold Spring Harb. Symp. Quant. Biol. *70*, 251–261.

Zimmermann, A. (2005). The emerging family of hepatoblastoma tumours: from ontogenesis to oncogenesis. Eur. J. Cancer *41*, 1503–1514.